

## Original papers

# A novel deep learning based approach for seed image classification and retrieval



Andrea Loddo<sup>\*</sup>, Mauro Loddo, Cecilia Di Ruberto

Department of Mathematics and Computer Science, University of Cagliari, via Ospedale 72, 09124 Cagliari, Italy

## ARTICLE INFO

**Keywords:**  
Agriculture  
Deep learning  
Machine learning  
Image analysis  
Seeds classification  
Retrieval

## ABSTRACT

Seeds image analysis has become essential to preserve biodiversity. This is why recognition and classification of plant species on the earth's planet is nowadays a great challenge. The paper focuses on this purpose by studying two plant seeds datasets to classify their families or species through deep learning techniques. SeedNet, a novel CNN has been proposed to face the depicted issue, and several state-of-the-art convolutional neural networks have been exploited for an exhaustive comparison of most adequate for the considered scenario. In detail, promising results in seed classification for both analysed datasets, reaching accuracy values of 95.65% for the first one and 97.47% for the second one, have been obtained. The retrieval problem with the deep learning approach was also addressed, achieving satisfying performances. We consider the obtained results for both the tasks as an excellent starting point to develop a complete seeds recognition, classification and retrieval system to offer impressive support in agriculture and botany fields.

## 1. Introduction

Thanks to its wide range of applications, image analysis plays an important role in the field of life sciences. Image analysis and processing methods are essential for understanding several medical characteristics or performing significant quantitative measurements on the images' objects. Haematology (Di Ruberto et al., 2020), biology (Campanile et al., 2019), and botany (Lo Bianco et al., 2017) are just some examples of application fields. Image analysis techniques have become more reliable with the development of fluorescence and high-resolution microscopes to gain biologists' interest. The possibility to study the structural details of biological elements, such as organisms and parts thereof deep, can have a profound impact on biological research. In general, it is an important research area in the agricultural domain for image classification, anomaly detection, and so on (Kamilaris and Pre-nafeta-Boldú, 2018). This work studies possible solutions to perform automatic feature extraction and classification from biological organisms belonging to Carpology; it is the discipline that studies spermatophyte seeds and fruits from both a morphological and a structural perspective. It is of fundamental importance for Paleobotanica, Paleo-environmental studies, and ecology if applied to remains of the past (Paleocarpology). Seeds image analysis techniques bring several advantages concerning the manual analysis. They can speed up the entire

process, reduce distortions induced by natural light and microscopes, and automatically classify the seed characteristics based on the image pixel values. The use of technology in agricultural work started at the beginning of the 20th century when the industry moved from animal-drawn tools to mechanised tools. Technological advances have contributed to an increase in discussions about the collection of large amounts of data that make up the environment of current information technology, given that data collection is not a new concept, particularly in the context of public data collection. More recently, scientists widely apply image analysis tools in plant sciences, e.g., to classify vascular plant species with the seeds' morphological and colourimetric features or to extract discriminative features from seeds images (Campanile et al., 2019). In detail, different systems to automatically identify plant species based on leaf recognition for plant cataloguing and preserving (Putzu et al., 2016; Di Ruberto and Putzu, 2014) have been proposed. In addition to that, some works (Lo Bianco et al., 2017Lo Bianco et al., 2017) regard botanical characterisation of germplasm. Ucchesu et al. (2015, 2016) aims to identify unknown plant seed in the archaeobotany field. At the same time, Sau et al. works (Sau et al., 2018Sau et al., 2019) are devoted to distinguishing group cultivars in the agronomy field. Operators acquire images through a digital camera or a flatbed scanner. Compared to the digital camera, the flatbed scanner offers the advantage to have a coherent illumination and a known image scale commonly

\* Corresponding author.

E-mail address: [andrea.loddo@unica.it](mailto:andrea.loddo@unica.it) (A. Loddo).

expressed in dots per inch (DPI) and providing quality and speed of workflow execution (Lind et al., 2012).

After the Convolutional Neural Network (CNN) AlexNet outbreak (Krizhevsky et al., 2012), many studies have been oriented to apply deep learning techniques to agriculture. Deep learning is a recent and modern technique for image processing and data analysis. It offers promising results and has great potential. Various fields successfully applied deep learning methods and, only recently, it has also joined the agriculture field. The applications of deep learning in agriculture are many, though recent ones, from the identification of herb types to the recognition of plants, from fruit counting to the classification of crop types. Many works in the literature deal with the classification and identification of areas of interest, including the detection of obstacles. Other studies concentrate on issues such as weed detection and soil analysis. Hall et al. (2015) propose a convolutional neural network to deal with the classification of leaves of different plant species, using a dataset of over 1,900 images divided into 32 species. We consider this to be the area closest to our work. Similarly, in Sladojevic et al. (2016), CaffeNet is used to identify leaf diseases in a database containing approximately 4,500 images, while Zhu et al. (2021) aim to recognise carrot appearance quality by training a Support Vector Machine (SVM) classifier with deep features, with excellent results from ResNet101 network. Deep learning is also used for identification and classification; in particular, AlexNet and GoogleNet are used to identify 14 species of crops and 26 diseases in Mohanty et al. (2016), while LeNet is used for diseased banana leaves in Amara et al. (2017). Other works concern the classification of different types of crops. In Kussul et al. (2017), the research focuses on the classification of wheat, corn, soybeans, sunflower, and sugar beet crops using CNN produced by the authors. In Krogh Mortensen et al. (2016), the authors use a modified version of VGG16 to identify oil crops, radishes, barley, grass, and weeds. Rebetez in Rebetez et al. (2016) classifies various crop styles from drone images using CNN and HistNN (an RGB histogram). To the best of our knowledge, no study involved deep learning approaches to classify single seeds. A very recent work (Gulzar et al., 2020) deals with the classification of seeds by CNN and transfer learning, even though the authors addressed the problem of seeds belonging to different phyla or classes starting from a set of the seeds. Przybylo and Jablonski (2019) focuses on acorn classification based on colour and intensity of the image of sections of the seeds as a feature. The authors obtain an accuracy of 85%, which is comparable to a manual assessment of the viability of oak seeds with a CNN strategy. Moreover, they investigate the impact of various image representations (colour, entropy, edges) and network architecture and its parameters on the classification results. On the contrary, our work aims to classify single seeds belonging to the same class or family, in which colour, shape, and texture differences can be much more unnoticeable.

The research here presented focuses on studying plant seed datasets from two points of view: their classification, based on the families or species they belong to, and their retrieval. Both tasks have been performed with a new proposed convolutional neural network architecture, and its results have been compared with either deep learning techniques and traditional approaches. Our contribution is fourfold: *i*) we propose **SeedNet**, a brand new CNN to perform classification and retrieval of seed images, which is accurate both in accuracy and training time; *ii*) we extensively compared our proposal with ten state-of-the-art CNNs; *iii*) we compared our CNN with four classical machine learning approaches, trained with handcrafted (HC) features; *iv*) we propose two brand new seed datasets of single crops, obtained with a concrete preprocessing step.

The rest of the paper is organised as follows. In Section 2, we describe our proposed CNN architecture, the employed dataset, the preprocessing methods used on both dataset images, and the conducted experiments. The experimental results, a discussion on classification and retrieval tasks, and a comparison between CNN-based and traditional approaches are given in Section 3.2. Finally, conclusions are drawn in Section 4.

## 2. Material and methods

In this work two datasets have been exploited, as described in Section 2.2.1 and 2.2.2. They contain heterogeneous seed images, both in number and characteristics. They are publicly available on request. Every dataset has been preprocessed as depicted in Section 2.3 and used for two different tasks: the classification of seeds family (or species) and the retrieval of similar seeds, given a query image containing a seed.

### 2.1. The proposed CNN architecture: SeedNet

Our study was mainly to propose a new model based on CNN, which provides an efficient and effective approach for single seed classification and retrieval. Our network architecture, SeedNet, contains six learnable layers, 5 of which are convolutional, and the last is fully-connected. The ReLU (Rectified Linear Unit) activation is applied to the output of every convolutional layer. Moreover, we periodically insert a pooling layer between successive convolutional layers, in order to reduce the amount of parameters and computation in the network, and hence to also control overfitting. More precisely, we employ a Max pooling strategy with a  $3 \times 3$  filter size, and  $1 \times 1$  stride. The input image size is  $224 \times 224 \times 3$ . According to the chosen dataset, the output of the last fully-connected layer is fed to a  $N$ -way softmax, which produces a distribution over the  $N$  class labels to predict, i.e. 6 for the Canadian and 23 for the local dataset. A detailed description of the CNN network is provided in Table 1. The network has proven to have the same accuracy performance as more complex and deeper networks but with a shallow training time, as shown in the next section.

### 2.2. Datasets

#### 2.2.1. Canadian dataset

The Canadian dataset is publicly available ([https://inspection.canada.ca/active/netapp/idseed/idseed\\_gallere.aspx?itemsNum=1&famkey=&family=&keyword=&letter=A](https://inspection.canada.ca/active/netapp/idseed/idseed_gallere.aspx?itemsNum=1&famkey=&family=&keyword=&letter=A)), and last updated in February 2019. It contains a significant number of seeds, organised in families, for 587 different images. Each image can contain from one to eight seeds, all belonging to the *Magnoliophyta* phylum. The dataset images are of different sizes ( $600 \times 800$  or  $600 \times 480$  or  $600 \times 400$ ). This dataset was chosen for its large population of families and cleanliness of the image backgrounds, which are fundamental factors to process them. In particular, for the experimentations we selected the families by considering the six most represented: *Amaranthaceae*, *Apocynaceae*, *Asteraceae*, *Brassicaceae*, *Plantaginaceae* and *Solanaceae*, for a total of 215 seed images. A sample of each family is shown in Fig. 1, while Table 2 reports the number of samples for family. A scale indicator characterises all the pictures, typically positioned in one of the corners, as shown in Fig. 5a, removed with a preprocessing step. It also aimed to produce a single image per seed to create a new dataset of cropped images, each containing a single seed. A detailed explanation is given in Section 2.3.

#### 2.2.2. Local dataset

The local dataset contains 3,386 samples of seeds from 120 plant species belonging to the *Fabaceae* family. This family was chosen because it is one of the most prominent ones and shows significant variability in the seeds' size and colouration. Fig. 2 shows two sample images. All samples come from the base collection in the Germplasm Bank of Sardinia (BG-SAR), University of Cagliari, Italy. During the acquisition, the operators arranged the seeds on the flatbed scanner, separating them from each other to avoid overlapping. Then the area occupied by the seeds has been covered with a tray lined with a blue background for the digital image, as shown in Fig. 3. The acquisition process used a minimum resolution of 400 dpi, and the resulting images are saved in the Joint Photographic Experts Group (JPEG) format with a resolution of  $2125 \times 2834$  (Vale et al., 2020). For our purposes, the

**Table 1**

Description of the proposed network, SeedNet.

Operation layer		Filters #	Size	Stride value	Activations	Layer #
Input Image		-	-	-	$224 \times 224 \times 3$	1
Convolutional Layer	Convolutional	64	$11 \times 11 \times 3$	$3 \times 3$	$75 \times 75 \times 64$	2
	ReLU	-	-	-	$75 \times 75 \times 64$	3
Pooling Layer	Max Pooling	1	$3 \times 3$	$1 \times 1$	$75 \times 75 \times 64$	4
	Convolutional	256	$5 \times 5 \times 64$	$3 \times 3$	$25 \times 25 \times 256$	5
Pooling Layer	ReLU	-	-	-	$25 \times 25 \times 256$	6
	Max Pooling	1	$3 \times 3$	$1 \times 1$	$25 \times 25 \times 256$	7
Convolutional Layer	Convolutional	256	$3 \times 3 \times 256$	$3 \times 3$	$9 \times 9 \times 256$	8
	ReLU	-	-	-	$9 \times 9 \times 256$	9
Pooling Layer	Max Pooling	1	$3 \times 3$	$1 \times 1$	$9 \times 9 \times 256$	10
	Convolutional	256	$3 \times 3 \times 256$	$3 \times 3$	$3 \times 3 \times 256$	11
Convolutional Layer	ReLU	-	-	-	$3 \times 3 \times 256$	12
	Max Pooling	1	$3 \times 3$	$1 \times 1$	$3 \times 3 \times 256$	13
Convolutional Layer	Convolutional	256	$3 \times 3 \times 256$	$3 \times 3$	$1 \times 1 \times 256$	14
	ReLU	-	-	-	$1 \times 1 \times 256$	15
Pooling Layer	Max Pooling	1	$3 \times 3$	$1 \times 1$	$1 \times 1 \times 256$	16
	Fully Connected	-	-	-	$1 \times 1 \times \text{No.ofClasses}$	17
Softmax Layer	Softmax	-	-	-	$1 \times 1 \times \text{No.ofClasses}$	18
	Classification Output	-	-	-	Class	19



(a) Amaranthaceae



(b) Apiaceae



(c) Asteraceae



(d) Brassicaceae



(e) Plantaginaceae



(f) Solanaceae

**Fig. 1.** Samples of seed for each species present in the Canadian dataset.**Table 2**

Canadian dataset description: family name and number of samples.

Family	Samples
Amaranthaceae	10
Apiaceae	56
Asteraceae	49
Brassicaceae	34
Plantaginaceae	43
Solanaceae	23

images containing the most numerous samples per species were selected and listed as follows: *Amorpha fruticosa*, *Anagyris foetida*, *Anthyllis barba jovis*, *Anthyllis cytisoides*, *Astragalus glycyphyllos*, *Calicotome villosa*, *Caragana arborescens*, *Ceratonia siliqua*, *Colutea arborescens*, *Cytisus purgans*, *Cytisus scoparius*, *Dorycnium pentaphyllum*, *Dorycnium rectum*, *Hedysarum coronarium*, *Lathyrus aphaca*, *Lathyrus ochrus*, *Medicago sativa*, *Melilotus*

*officinalis*, *Pisum sativum*, *Senna alexandrina*, *Spartium junceum*, *Trifolium angustifolium*, *Vicia faba*, for a total of 1,988 seeds, and 23 different species. A sample of each species is shown in Fig. 4, while Table 3 reports the number of samples for species.

Even from this dataset, the most numerous species were selected, similarly to the previous one, in which we selected the most represented families. The collectors acquired these seeds images on different backgrounds of various shades of blue. Consequently, it helps us find the best images to extract crops of single seeds with a preprocessing procedure.

### 2.3. Datasets preprocessing

The preprocessing step is designed to create a single image for each seed from the full-size images of both sets. We divided them into families for the Canadian dataset and into species for the local one. As already mentioned, for the Canadian dataset, the first preprocessing step was to remove the seed scale indicators. Then, the second step was to create binary seed masks. Thanks to the fairly uniform background, it was

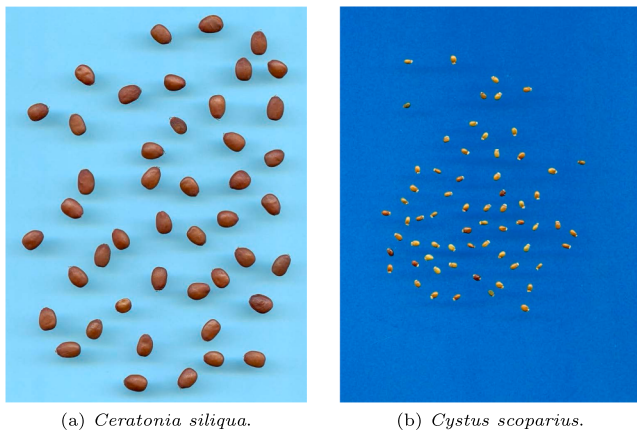


**Fig. 2.** Examples of seeds images present in the local dataset. They represent two different species: (a) contains *Ceratonia siliqua*, while (2b) contains *Cystus scoparius*.



**Fig. 3.** Local dataset images acquisition procedure. The operator arranged several seeds on the flatbed scanner.

possible to obtain the mask by identifying the highest peak of the image histogram, i.e. representing the background's intensity values, and excluding them from the image according to a range of 5%. In Fig. 5 the results of this step are depicted.

However, the obtained binary mask could contain more than one seed. Consequently, we used it to identify the bounding boxes of each seed. Moreover, the mask could also contain portions of other close seeds and so included in the same bounding box. The most significant region in this image represents the relevant seed, i.e. the seed of interest. Thanks to the mask of the seed of interest, it was possible to get the image corresponding to the main seed by taking the background pixel value and substituting the cropped seed image's pixel values that do not match the mask. The final image is then the seed image, ready to be given as input to a CNN. Fig. 6 depicts the results of this process step-by-step.

On the other hand, as regards the local dataset, the work was more straightforward. Firstly, it was not possible to use the same histogram-based method employed with the Canadian set due to the presence of fairly marked shadows that did not allow to generate clean masks. However, all the images background have been acquired with various shades of blue (see Fig. 7). Therefore, it was possible to isolate the Blue value of the RGB images to get pure masks with an automatic thresholding procedure, as indicated in our previous work (Vale et al., 2020). It is also important to note that, during the acquisition step, the seeds were

well spaced from each other. As a consequence, the bounding box of each region allowed to create a single image for every seed. We discarded some species due to the low sharpness and excessively small size of the seeds. Fig. 7 show an original sample image with its derived binary mask and some seed images extracted from it.

### 3. Results and discussion

We now describe the experimentation conducted in this work. In detail, in Section 3.1 we first describe the experimental setup adopted for the classification and retrieval tasks. Then, we report the results of the experiments performed on both datasets and tasks with SeedNet, compared to existing CNNs (Section 3.2). After a further comparison of deep vs machine learning methods in Section 3.3, we give a detailed discussion of the obtained results in Section 3.4.

#### 3.1. Setup

##### 3.1.1. Seed image classification via deep learning

The images to classify have a uniform background and contain only one seed. They are organised into classes that are families for the Canadian dataset and species for the local dataset. Even if numerous, the images are subjected to an augmentation process, i.e., geometric transformations (rotations, translations, or resizing), to increase the dataset's size. The dataset is also divided into three parts, one for the training (80% of the images), one for the validation (10% remaining), and 10% for testing. No randomisation strategy has been applied in order to make the experiments reproducible. The validation set is used to provide an unbiased evaluation of a model fit on the training set while tuning model hyperparameters. The validation set results are then used to update higher level hyperparameters. So the validation set affects a model, but only indirectly. Finally, the test set is used to provide an unbiased evaluation of a final model fit on the training set. The tests were carried out both on SeedNet and on several popular CNNs to find the best architecture for our purpose. The tested networks are AlexNet (Krizhevsky et al., 2012), the Residual Networks (He et al., 2016) ResNet18, ResNet50, ResNet101, GoogLeNet (Szegedy et al., 2015), ShuffleNet (Zhang et al., 2018), SqueezeNet (Iandola et al., 2016), MobileNetV2 (Sandler et al., 2018), InceptionV3 (Szegedy et al., 2016) and VGG16 (Simonyan and Zisserman, 2015). The experiments were performed using the same training options for all networks to evaluate the performance differences. All the simulations were executed using the same solver, i.e., Adam, to achieve better performance than other algorithms. Other standard training options are the Learning Rate equal to 1,00E-04 and Validation Frequency equal to 5.

**Metrics.** The performance measures have been evaluated by averaging on five different simulations for all the networks. The measures used to quantify the performance of a network are the Accuracy (Acc), specificity (Spec), and sensitivity (Sen), as following defined:

$$\text{Accuracy} = \frac{TP + TF}{TP + TF + FP + FN}, \quad (1)$$

$$\text{Specificity} = \frac{TN}{FP + TN}, \quad (2)$$

$$\text{Sensitivity} = \frac{TP}{TP + FN}. \quad (3)$$

The specificity measures the proportion of negatives that are correctly identified (also called true negative rate). The sensitivity measures the proportion of positives that are correctly identified (also called true positive rate). The third measure is the accuracy, defined as the correctly labelled instances ratio to the whole pool of instances. We also evaluated the accuracy's standard deviation to test the stability of each network.

Finally, as we face a multi-class imbalanced problem, three of the most common global metrics for multi-class imbalance learning to



**Fig. 4.** Sample of seed for each species present in the local dataset.

**Table 3**  
Local dataset description: species name and number of samples.

Species	Samples	Species	Samples
<i>Amorpha fruticosa</i>	51	<i>Dorycnium rectum</i>	236
<i>Anagyris foetida</i>	29	<i>Hedysarum coronarium</i>	208
<i>Anthyllis barba jovis</i>	51	<i>Lathyrus aphaca</i>	52
<i>Anthyllis cytisoides</i>	29	<i>Lathyrus ochrus</i>	46
<i>Astragalus glycyphyllos</i>	50	<i>Medicago sativa</i>	116
<i>Calicotome villosa</i>	32	<i>Melilotus officinalis</i>	176
<i>Caragana arborescens</i>	36	<i>Pisum sativum</i>	121
<i>Ceratonia siliqua</i>	45	<i>Senna alexandrina</i>	194
<i>Colutea arborescens</i>	42	<i>Spartium junceum</i>	109
<i>Cytisus purgans</i>	44	<i>Trifolium angustifolium</i>	183
<i>Cytisus scoparius</i>	65	<i>Vicia faba</i>	31
<i>Dorycnium pentaphyllum</i>	42		

evaluate the networks performance (Alejo et al., 2013) were applied. They are the macro average geometric (MAvG), defined as the geometric average of the partial accuracy of each class, the macro average arithmetic (MAvA), defined as the arithmetic average of the partial accuracies of each class, and the mean F-measure (MFM). We describe them as follows:

$$MAvG = \left( \prod_{i=1}^J Acc_i \right)^{\frac{1}{J}}, \quad (4)$$

$$MAvA = \frac{\sum_{i=1}^J Acc_i}{J} \quad (5)$$

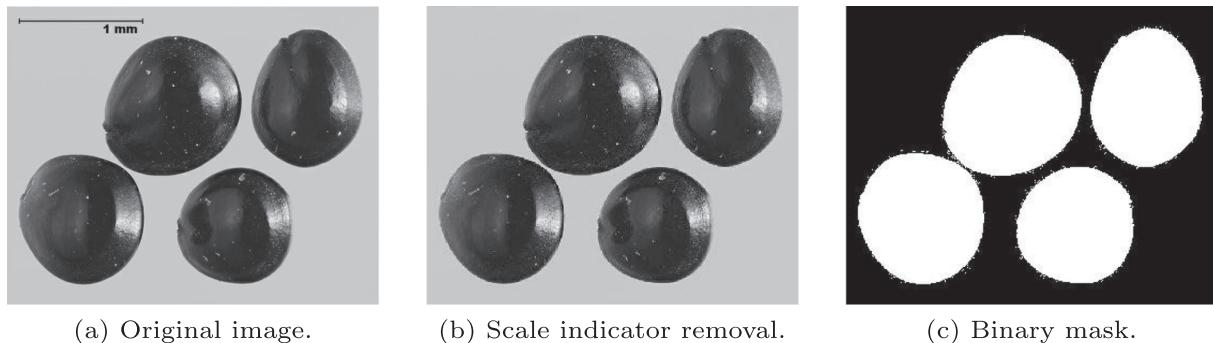
$$MFM = \sum_{i=1}^J \frac{2(Precision \cdot Sensitivity)}{Precision + Sensitivity} \quad (6)$$

with Precision defined as follows:

$$Precision = \frac{TP}{TP + FP} \quad (7)$$

### 3.1.2. Seed image retrieval via deep learning

Beyond the classification task, we verified the possibility of using convolutional neural networks for seed image retrieval and evaluated their performances. Generally, a content-based image retrieval system searches and retrieves images based on the visual contents of the images, i.e. features such as colour, texture, shape, and spatial layout. CNNs can replace traditional feature extractors since they have a solid ability to extract complex features that express the image in much more detail. So,

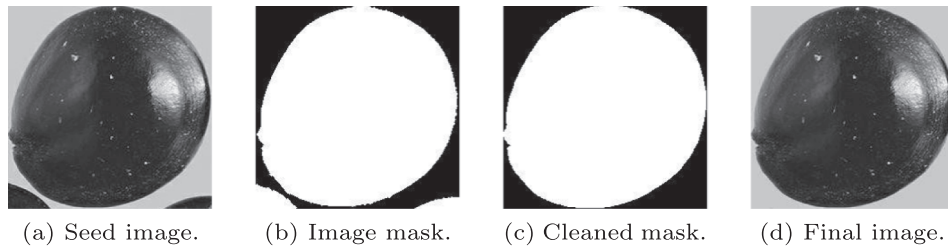


(a) Original image.

(b) Scale indicator removal.

(c) Binary mask.

**Fig. 5.** Binary seed image creation process from the Canadian database. All the images contains a scale indicator, as shown in (a). (b) shows the image after the first preprocessing step, and (c) shows the final binary mask.



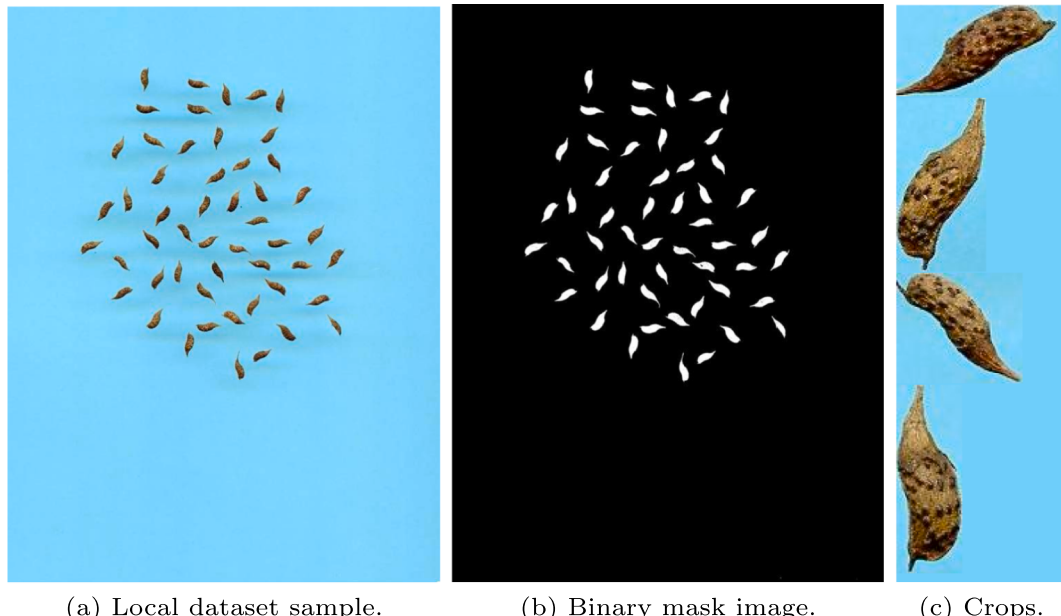
(a) Seed image.

(b) Image mask.

(c) Cleaned mask.

(d) Final image.

**Fig. 6.** Single seed image creation process from the Canadian database. From left to right: cropped seed image in (a); (b) and (c) show the cropped seed image mask and the main cropped seed image mask, respectively. The final obtained seed image is (d).



(a) Local dataset sample.

(b) Binary mask image.

(c) Crops.

**Fig. 7.** A sample from the local dataset containing *Amorpha fruticosa* species. From left to right, (a) shows the original image; (b) its related binary mask. Finally, (c) represents four crop examples extracted from (d).

they can be used for feature extraction, and the extracted features can be utilized for retrieval. All the networks already employed for classification have been tested for the new task, too, with the addition of VGG19. It is extendedly employed for features extraction (Mateen et al., 2019). The features were extracted from the last fully connected layer unless AlexNet. For it, we reported the penultimate layer because it provided us with the best results. The extracted features are then arranged as multidimensional feature vectors, used to construct the database of features.

**Similarity measures.** For similarity distance measurement, many

methods have been developed. Here, we have utilized both Euclidean distance and  $D_1$  distance (Dubey et al., 2015). The  $D_1$  similarity measure used to compare the feature vectors of two images is defined as:

$$D_1(t, DB_s) = \sum_{\tau=1}^{\dim} \left| \frac{F^{DB_s}(\tau) - F^t(\tau)}{1 + F^{DB_s}(\tau) - F^t(\tau)} \right| \quad (8)$$

where  $\dim$  is the dimension of the feature vectors,  $F^t(\tau)$  is the  $\tau^{th}$  element of the feature vector of the query image  $t$  and  $F^{DB_s}(\tau)$  is the  $\tau^{th}$  element of the feature vector of the  $s^{th}$  image in the database  $DB$ .

**Metrics.** Four performance measures, namely average retrieval precision, *ARP*, average retrieval rate, *ARR*, *F<sub>score</sub>* and mean average precision, *mAP*, have been used to compare the retrieval performances. The mathematical formulation for each of these performance measures is given as follows:

$$\text{ARP} = \frac{\text{number of relevant images retrieved}}{\text{total number of images retrieved}(\eta)} = \frac{100}{\omega} \sum_{i=1}^{\omega} \frac{r(DB_i)}{\eta} \quad (9)$$

$$\text{ARR} = \frac{\text{number of relevant images retrieved}}{\text{total number of relevant images in the database}} = \frac{100}{\omega} \sum_{i=1}^{\omega} \frac{r(DB_i)}{g(DB_i)} \quad (10)$$

$$F_{\text{score}} = \frac{2 \times \text{ARP} \times \text{ARR}}{\text{ARP} + \text{ARR}} \quad (11)$$

$$mAP = \frac{100}{\omega} \sum_{i=1}^{\omega} \sum_{\eta=1}^{g(DB_i)} \frac{r(DB_i)}{\eta} \quad (12)$$

where  $\omega$  denotes the image count in the database  $DB$ ,  $r(DB_i)$  and  $g(DB_i)$  are the number of relevant retrieved images and the number of relevant ground truth images available for the  $i^{\text{th}}$  query image of  $DB$ , respectively. During the experiments, every image in the database is used as a query image and is matched with every remaining image in the database.

### 3.2. Results

#### 3.2.1. Classification results

We used a six-class subset for our experimentations on the Canadian dataset, as described in Section 2.2.1. For this dataset, the task was to classify the different families of the *Magnoliophyta* phylum. As already mentioned, the tests were carried out on several CNNs using the same training options, particularly the same mini-batch size and the number of epochs. Table 4 shows the results of the tests performed on all the listed networks.

Regarding the local dataset experiments, we used a twenty-three-class subset, as described in Section 2.2.2. The task was to classify the different species of the *Fabaceae* family. We carried out the tests using all the networks employed in the previous dataset experiments, with the same training options. Table 5 shows the obtained numerical results.

#### 3.2.2. Retrieval results

The retrieval experiments ensued the following strategy: every image is used as a query image and is matched with every remaining image in the database. Tables 6 and 7 present the retrieval performances of all the networks in terms of the four considered measures by choosing the top 100 matches, i.e.  $\eta = 100$ , and the two chosen similarity distances.

### 3.3. Deep learning vs traditional machine learning comparison

A comparison of deep learning approaches with traditional machine

learning methods, provided with handcrafted features, was also realised. Three categories of HC features have been considered: 32 shape structure, 16 texture information, and 16 colour intensity values, for a total amount of 64 descriptors. Among the texture ones, we also exploited the Gray-Level Co-Occurrence Matrix (GLCM) (Haralick et al., 1973), which describes the pairwise arrangement of pixels with the same grey level, to extract information of local similarities. More precisely, we extracted the following second-order statistics: energy, contrast, correlation and homogeneity. The HC features have been extracted from the pre-processed images using our previously proposed seed analysis ImageJ plugin (Loddo et al., 2021). Subsequently, we used them as inputs to four classification models: KNN, Naive Bayes, Random Forest, and Support Vector Machine. Naive Bayes classifiers are probabilistic models based on applying Bayes' theorem with strong independence assumptions between the features. KNN uses the  $k$  closest training examples in the dataset as inputs, and a voting strategy of the neighbours classifies an object. SVM is a non-probabilistic binary linear classifier that assigns objects to a category, mapping examples to points in space to maximise the width of the gap between categories. Finally, Random Forest consists of a large number of individual decision trees that operate as an ensemble. Each tree provides a class prediction, and the class with the most votes is the model prediction.

Considering the complexity of our selected feature spaces, we selected these classifiers in order to guarantee accuracy, flexibility and adaptation to the data. All of the described features were fed to the four classifiers by using the Weka package tool (Hall et al., 2009). Each classifier was trained with 10-fold cross-validation to guarantee training sets variability and, for each scenario, the model with the largest area under the ROC curve (AUC) was chosen. Table 8 shows the classification results on both datasets.

We performed comparisons with the features extracted from SeedNet for what concerns the adaptability of the traditional features to the context of seed image retrieval. The same distances and metric measurements already depicted in Section 3.1.2 were used. Table 9 shows the retrieval performances of the HC descriptors in terms of the four considered measures, by choosing the top 100 matches, i.e.  $\eta = 100$ , and the two similarity distances, namely Euclidean and  $D_1$ .

### 3.4. Discussion

Regarding the classification results obtained with the CNNs on the Canadian dataset, as it can be seen in Table 4, AlexNet, ResNet18, ResNet50 and, most of all, our proposed model are the networks that achieved the best compromise between classification performances, stability, and training speed. Besides, they also resulted in being the best in dealing with the unbalanced multi-class problem. InceptionV3 also has outstanding performances against a shallow training time. Similar performances are reached by ShuffleNet, with the advantage of a faster training time and improved stability. Finally, among the other networks, VGG16, despite the large number of levels that should increase the efficiency, showed a decline in performance with relatively high standard

**Table 4**

Summary of the experimentation results on the Canadian dataset (StD is the deviation standard of Acc value and Time is the training time in minutes).

Network	Acc	Spec	Sen	MAvG	MFM	MAvA	StD	Time
AlexNet	<b>95.65</b>	96.67	96.67	96.35	96.30	96.67	5.21	22
ResNet18	<b>95.65</b>	97.22	94.44	<b>97.01</b>	95.15	<b>97.22</b>	3.89	30
ResNet50	<b>95.65</b>	96.67	94.44	96.35	<b>94.82</b>	96.67	1.73	77
ResNet101	91.30	88.33	91.11	85.84	87.41	88.33	4.26	118
GoogLeNet	86.96	90.28	87.78	89.70	88.08	90.28	3.06	32
ShuffleNet	91.30	91.88	80.83	78.05	77.38	80.88	1.73	24
SqueezeNet	78.26	88.10	78.89	86.13	78.32	88.10	3.47	15
MobileNetV2	86.96	91.67	85.56	90.67	<b>84.97</b>	91.67	2.13	55
InceptionV3	91.30	<b>93.89</b>	93.33	93.45	92.93	93.89	3.25	103
VGG16	78.26	81.67	82.50	80.39	81.32	81.67	5.21	160
SeedNet	95.24	<b>98.96</b>	<b>97.22</b>	<b>97.01</b>	<b>96.97</b>	<b>97.22</b>	<b>1.73</b>	4

**Table 5**

Summary of the experimentation results on the local dataset (StD is the deviation standard of Acc value and Time is the training time in minutes).

Network	Acc	Spec	Sen	MAvG	MFM	MAvA	StD	Time
AlexNet	93.43	91.08	91.36	90.15	90.51	91.08	5.21	74
ResNet18	<b>97.47</b>	96.63	95.50	96.11	95.46	96.63	2.49	34
ResNet50	96.46	94.44	94.98	96.15	95.20	96.44	0.59	34
ResNet101	96.97	96.61	94.66	96.34	94.71	96.61	2.86	125
GoogLeNet	95.45	95.06	93.47	94.67	93.16	95.06	1.83	21
ShuffleNet	96.46	95.90	94.37	95.57	94.55	95.90	1.29	18
SqueezeNet	95.96	95.75	94.71	95.13	94.84	95.75	3.47	23
MobileNetV2	93.94	93.16	91.51	92.67	91.85	93.16	1.02	33
InceptionV3	96.46	95.99	94.81	95.74	95.02	95.99	3.25	290
VGG16	95.96	94.82	94.86	94.22	94.25	94.82	4.21	224
SeedNet	<b>97.47</b>	<b>99.88</b>	<b>96.81</b>	<b>96.60</b>	<b>96.98</b>	<b>96.81</b>	<b>0.59</b>	<b>12</b>

**Table 6**

Performance comparison of the networks in terms of ARP, ARR,  $F_{score}$  and mAP for top 100 matches (i.e.  $\eta = 100$ ) and Euclidean distance.

Network	Canadian dataset				Local dataset			
	ARP	ARR	$F_{score}$	mAP	ARP	ARR	$F_{score}$	mAP
AlexNet	19.4	47.7	27.6	34.6	<b>43.7</b>	32.1	37.0	<b>46.8</b>
VGG16	17.7	44.8	25.4	33.3	38.2	33.3	35.6	44.0
VGG19	17.1	45.8	17.1	34.6	37.1	31.4	34.0	40.0
ResNet18	16.9	47.7	25.0	35.4	36.7	30.1	33.1	38.4
ResNet50	18.0	46.0	25.9	35.7	41.9	32.7	36.7	45.2
Resnet101	17.7	45.3	25.5	34.0	34.5	31.9	33.2	39.9
GoogLeNet	18.0	45.3	25.5	31.6	33.2	29.7	31.4	36.4
ShuffleNet	18.0	45.5	25.8	33.8	37.5	30.5	33.6	39.8
SqueezeNet	17.2	42.3	24.5	31.0	42.4	34.1	<b>37.8</b>	45.9
MobileNetV2	13.6	37.7	20.0	27.7	37.3	34.3	35.7	42.1
InceptionV3	19.4	52.1	28.3	<b>40.7</b>	31.2	28.2	29.6	33.3
SeedNet	<b>23.9</b>	<b>54.0</b>	<b>33.1</b>	37.0	35.3	28.7	31.7	38.0

**Table 7**

Performance comparison of the networks in terms of ARP, ARR,  $F_{score}$  and mAP for top 100 matches (i.e.  $\eta = 100$ ) and  $D_1$  distance.

Network	Canadian dataset				Local dataset			
	ARP	ARR	$F_{score}$	mAP	ARP	ARR	$F_{score}$	mAP
AlexNet	16.2	40.2	23.1	25.1	31.4	22.3	26.1	27.7
VGG16	16.6	42.4	23.9	29.7	27.5	22.4	24.7	24.3
VGG19	15.0	37.5	21.4	25.4	23.8	20.9	22.3	21.2
ResNet18	17.3	42.4	24.6	26.0	22.7	20.1	21.3	21.1
ResNet50	14.5	37.0	20.8	23.2	29.0	24.2	26.4	26.7
ResNet101	15.5	37.6	22.0	23.6	27.9	23.2	25.3	25.9
GoogLeNet	14.6	36.3	20.8	21.7	25.7	22.8	24.2	23.2
ShuffleNet	15.9	38.0	22.4	24.9	30.7	20.4	24.5	24.5
SqueezeNet	16.8	43.4	24.2	31.2	29.7	<b>28.9</b>	29.3	33.5
MobileNetV2	16.0	39.7	22.8	24.3	25.8	19.7	22.3	20.5
InceptionV3	15.8	39.8	22.6	24.2	23.9	18.4	20.8	18.7
SeedNet	<b>17.8</b>	<b>43.6</b>	<b>25.3</b>	<b>30.8</b>	<b>37.6</b>	27.8	<b>32.0</b>	<b>35.2</b>

**Table 8**

Performance results attained using HC descriptors and traditional classifiers on Canadian and local dataset, compared to the proposed CNN. DS indicates the dataset, while time is the training time, expressed in seconds, except for the CNN, which is expressed in minutes.

DS	Classifier	Acc	Spec	Sen	MAvG	MFM	MAvA	Time
Canada	kNN	94.88	93.45	90.65	93.34	91.64	93.45	<b>0.4</b>
	Naive Bayes	91.63	90.87	89.88	90.77	90.32	90.87	6
	Random Forest	93.02	91.38	88.18	91.25	89.34	91.38	2
	SVM	94.88	94.75	91.06	94.61	92.44	94.75	1
	SeedNet	<b>95.24</b>	<b>98.96</b>	<b>97.22</b>	<b>97.01</b>	<b>96.97</b>	<b>97.22</b>	4 m
Local	kNN	80.54	76.59	74.70	74.72	75.15	76.59	8
	Naive Bayes	85.16	81.78	84.82	79.68	82.76	81.78	64
	Random Forest	93.76	94.55	89.75	94.37	91.39	94.55	29
	SVM	85.66	83.85	78.88	82.56	80.58	83.85	18
	SeedNet	<b>97.47</b>	<b>99.88</b>	<b>96.81</b>	<b>96.60</b>	<b>96.98</b>	<b>96.81</b>	12 m

**Table 9**

Retrieval performance results comparison using HC descriptors vs SeedNet's extracted features on Canadian and local dataset, by choosing the top 100 matches, i.e.  $\eta = 100$ . Note that SM stands for Similarity Measure, and EUC indicates the Euclidean distance.

SM	Descriptor	Canadian dataset				Local dataset			
		ARP	ARR	$F_{score}$	mAP	ARP	ARR	$F_{score}$	mAP
EUC	HC	22.3	<b>55.6</b>	31.8	<b>45.7</b>	10.7	9.5	10.1	10.2
	SeedNet	<b>23.9</b>	54.0	<b>33.1</b>	37.0	<b>35.3</b>	<b>28.7</b>	<b>31.7</b>	<b>38.0</b>
D1	HC	<b>23.5</b>	<b>54.8</b>	<b>32.9</b>	<b>41.6</b>	20.4	14.7	17.1	16.2
	SeedNet	17.8	43.6	25.3	30.8	<b>37.6</b>	<b>27.8</b>	<b>32.0</b>	<b>35.2</b>

deviations to confirm their instability. It is important to emphasise that the proposed network reaches the best classification performance and is also characterised by the lowest training time.

For the classification task on the local dataset, Table 5 shows that the best performing networks are our proposed CNN and ResNet18, both in terms of accuracy and in dealing with the class unbalance. However, ResNet18 presents a slight instability. All the other networks achieved similar and outstanding performances. In particular, InceptionV3 and VGG16 show the slowest training phase. In conclusion, also in this experimentation, SeedNet proved to be the best both in terms of performance and speed.

As expected for the retrieval task performed with deep features, the similarity measure influences the retrieval performances, and for our problem, the best one seems to be the Euclidean distance (See Table 6 and 7). Even a little less effective than for classification, the results can be considered satisfying and confirm the potential use of deep learning techniques for retrieval tasks. Overall, our proposed model turns out to be the most performing among the considered networks.

Finally, in order to make our experiments more exhaustive, we performed several comparisons with traditional machine learning methods for both classification and retrieval tasks. Regarding classification one, as expressed in Table 8, the SVM reached the best results in every metric for the Canadian datasets, even though all the classifiers achieved results higher than 90%, showing that the chosen features are representative for the entire six-classes dataset. However, looking at the local dataset results, Random Forest is the only classifier that exceeds 90% in every metric except for sensitivity, showing its excellent flexibility in this twenty-three-classes scenario.

Although the satisfactory results of traditional classifiers, no one outperformed SeedNet. CNNs methods generally achieved better performances than the traditional classifiers, which nevertheless had training times less than or equal to a minute. Our proposed model also required 4 and 12 times the training time on the Canadian and local dataset, respectively, even though it outperformed every single compared CNN.

About the retrieval performances of the HC descriptors, Table 9 shows that the choice of the similarity measure influences the retrieval performances, as already happened for the CNN descriptors. In this case, the  $D_1$  distance reached the best overall results, even though they are pretty similar in Canadian dataset retrieval.  $D_1$  distance is undoubtedly better in local dataset retrieval. From the comparison, we can confirm how the CNN descriptors can be appropriate for seed images retrieval. However, they are not the best in every analysed scenario, in contrast to the classification results. In detail, focusing on the  $F_{score}$  metric for the Canadian dataset, we can state that the CNN descriptors outperform the traditional ones, obtaining 33.1% against 31.8%, respectively, using the Euclidean distance. However, with the same configuration and the  $D_1$  distance, the traditional descriptors outperform the CNN ones, reaching 32.9% and 25.3%, respectively. Regarding the local dataset, the CNN descriptors outperform the traditional ones for both distance metrics. Specifically, all the CNN descriptors reached a way higher  $F_{score}$  value than the traditional ones. In summary, considering the comparison between the two types of descriptors, we can confirm that the CNN descriptors can be adapted for retrieval task, and, in general, they outperform the HC descriptors, significantly improving the overall

retrieval measurements.

To sum up, SeedNet seems robust for both tasks, reaching outstanding performance results with both datasets and having a low training time if compared to the other examined networks. However, other CNNs obtained satisfactory results, like the Residual Networks (e.g. ResNet18) in both tasks, or SqueezeNet in the retrieval one. The CNNs are also generally preferable in performances with respect to the traditional methods, even though the last ones reached interesting results with low training times.

#### 4. Conclusions

In this work, we mainly focused to realise and propose a brand new CNN architecture for seed images classification and retrieval tasks, named SeedNet. In addition to it, we studied the performances of different CNNs and compared them against our CNN model for both tasks by using two very different datasets. The aim was to evaluate the possibility to find the architecture of the best performing model and the best training options for these issues. We also compare deep against traditional machine learning methods, trained with handcrafted features, for both tasks.

Of course, some aspects can strongly influence the whole classification or retrieval task. First of all, the quality of the original images to process before being analysed by a network. Secondly, the preprocessing step, such as the background cleaning, the spacing of the seeds during the acquisition, and, finally, the size of the seeds present in the images. Last but not least is the imbalance of categories of both the datasets.

During the experimentation, the most efficient solver for classification turned out to be Adam, as Sgdm experienced drops in performance. The experimental results show a correlation between the number of CNN levels and its performance, with some important exceptions. Above all, VGG16 produced relatively low performances. Considering that it is now commonly used as a backbone network, it can be avoided in such a scenario. Secondly, our proposed model and ResNet18 obtained excellent performances in both experimentations, even though they do not contain a high number of levels. They are both eligible as the best networks for this study. Our experiments permit us to deduce that, regarding the classification task, the best CNNs are our proposed model, ResNet50 and ResNet18, achieving outstanding performances with acceptable stability, low training time, and high ability to manage the class unbalance. For what concerns the retrieval task, overall, our model reached the best results. The lower retrieval values in the local dataset are certainly due to the fact that it contains seeds of different species belonging to the same family, while the Canadian dataset is composed of seeds of different families. Consequently, the visual content of an image used in the retrieval process is much less discriminative in the local dataset than in the Canadian one.

Considering the comparison between the CNN approaches and traditional machine learning methods, the CNN descriptors outperformed the traditional descriptors, both in classification and retrieval. As a future direction, we are planning to investigate the most promising networks deeply. The purpose is to evaluate potential modifications of their architecture to consider the depicted scenario and use larger datasets for the experimentations. Then, we would like to extend our approach to distinguish among seeds' genus and variety. Moreover,

we plan to combine deep and traditional descriptors to investigate possible retrieval performance improvements, particularly on the local dataset. Finally, as regarding the retrieval task, it could be interesting to propose a metric learning approach to find the most suitable similarity metrics for this task. In conclusion, we can affirm that deep learning techniques generally have substantial potential for the classification and retrieval of seed images.

## 5. Authors contribution

Conceptualization, A.L. and C.D.R.; methodology, A.L. and C.D.R.; software, A.L. and M.L.; validation, A.L., M.L. and C.D.R.; formal analysis, A.L. and C.D.R.; investigation, A.L., M.L. and C.D.R.; resources, A.L., M.L. and C.D.R.; data curation, A.L., M.L. and C.D.R.; writing—original draft preparation, A.L. and C.D.R.; writing—review and editing, A.L., M.L. and C.D.R.; supervision, C.D.R.. All authors have read and agreed to the published version of the manuscript.

## 6. Funding

The Regione Autonoma della Sardegna partially supported the research in this paper with the research project “Algorithms and Models for Imaging Science [AMIS]” (finanziato con risorse FSC 2014–2020 Patto per lo Sviluppo della Regione Sardegna).

## 7. Abbreviations

The following abbreviations are used in this manuscript:

DPI	Dots Per Inch
CNN	Convolutional Neural Network
JPEG	Joint Photographic Experts Group
HC	Handcrafted
Acc	Accuracy
Spe	Specificity
Sen	Sensitivity
MAvG	Macro Average Geometric
MFM	Mean F-Measure
MAvA	Macro Average Arithmetic
Std	Accuracy's standard deviation
ARP	Average Retrieval Precision
ARR	Average Retrieval Rate
mAP	mean Average Precision
SVM	Support Vector Machine
KNN	K Nearest Neighbour
RF	Random Forest
GLCM	Gray-Level Co-Occurrence Matrix
AUC	Area Under the ROC Curve
TP	True Positive
FP	False Positive
TN	True Negative
FN	False Negative.

## Declaration of Competing Interest

The authors declare that they have no known competing financial interests or personal relationships that could have appeared to influence the work reported in this paper.

## Declaration of Competing Interest

The authors declare that they have no known competing financial interests or personal relationships that could have appeared to influence the work reported in this paper.

## References

- R. Alejo, J.A. Antonio, R.M. Valdovinos, J.H. Pacheco-Sánchez, Assessments metrics for multi-class imbalance learning: A preliminary study, in: Pattern Recognition - 5th Mexican Conference, MCPR 2013, Querétaro, Mexico, June 26–29, 2013.
- Proceedings, Vol. 7914 of Lecture Notes in Computer Science, Springer, 2013, pp. 335–343. doi:10.1007/978-3-642-38989-4\_34.
- J. Amara, B. Bouaziz, A. Algergawy, A deep learning-based approach for banana leaf diseases classification, in: Datenbanksysteme für Business, Technologie und Web (BTW 2017), 17. Fachtagung des GI-Fachbereichs, Datenbanken und Informationssysteme (DBIS), 6–10. März 2017, Stuttgart, Germany, Workshopband, Vol. P-266 of LNI, GI, 2017, pp. 79–88.
- G. Campanile, C.D. Ruberto, A. Loddo, An open source plugin for image analysis in biology, in: S. Reddy (Ed.), 28th IEEE International Conference on Enabling Technologies: Infrastructure for Collaborative Enterprises, WETICE 2019, Naples, Italy, June 12–14, 2019, IEEE, 2019, pp. 162–167. doi:10.1109/WETICE.2019.00042.
- Di Ruberto, C., Loddo, A., Putzu, L., 2020. Detection of red and white blood cells from microscopic blood images using a region proposal approach. Comput. Biol. Med. 116, 103530. <https://doi.org/10.1016/j.combiomed.2019.103530>.
- Dubey, S., Singh, S., Singh, R., 2015. Local diagonal extrema pattern: a new and efficient feature descriptor for ct image retrieval. IEEE Signal Process Lett. 22, 1215–1219. <https://doi.org/10.1109/LSP.2015.2392623>.
- Gulzar, Y., Hamid, Y., Soomro, A.B., Alwan, A.A., Journaux, L., 2020. A convolution neural network-based seed classification system. Symmetry 12, 1–18. <https://doi.org/10.3390/sym12122018>.
- Hall, M., Frank, E., Holmes, G., Pfahringer, B., Reutemann, P., Witten, I.H., 2009. The WEKA data mining software: an update. SIGKDD Explorations 11 (1), 10–18.
- Hall, D., McCool, C., Dayoub, F., Sunderhauf, N., Upcroft, B., 2015. Evaluation of features for leaf classification in challenging conditions. IEEE Winter Conference on Applications of Computer Vision 2015, 797–804. <https://doi.org/10.1109/WACV.2015.111>.
- Haralick, R.M., Shanmugam, K., Dinstein, I., 1973. Textural features for image classification. IEEE Transactions on Systems, Man, and Cybernetics SMC-3 (6), 610–621. <https://doi.org/10.1109/TSMC.1973.4309314>.
- K. He, X. Zhang, S. Ren, J. Sun, Deep residual learning for image recognition, in: 2016 IEEE Conference on Computer Vision and Pattern Recognition, CVPR 2016, Las Vegas, NV, USA, June 27–30, 2016, IEEE Computer Society, 2016, pp. 770–778. doi: 10.1109/CVPR.2016.90.
- Kamilaris, A., Prenafeta-Boldú, F.X., 2018. Deep learning in agriculture: A survey. Computers and Electronics in Agriculture 147, 70–90. <https://doi.org/10.1016/j.compag.2018.02.016>.
- Krizhevsky, A., Sutskever, I., Hinton, G.E., 2012. Imagenet classification with deep convolutional neural networks. In: Bartlett, P.L., Pereira, F.C.N., Burges, C.J.C., Bottou, L., Weinberger, K.Q. (Eds.), Advances in Neural Information Processing Systems 25: 26th Annual Conference on Neural Information Processing Systems 2012, Proceedings of a meeting held December 3–6, 2012, Lake Tahoe, Nevada, United States, pp. 1106–1114.
- Kussul, N., Lavreniuk, M., Skakun, S., Shelestov, A., 2017. Deep learning classification of land cover and crop types using remote sensing data. IEEE Geosci. Remote Sens. Lett. 14 (5), 778–782. <https://doi.org/10.1109/LGRS.2017.2681128>.
- Lind, R., 2012. Open source software for image processing and analysis: picture this with imagej. In: Harland, L., Forster, M. (Eds.), Open Source Software in Life Science Research, Woodhead Publishing Series in Biomedicine. Woodhead Publishing, pp. 131–149. <https://doi.org/10.1533/9781908818249.131>.
- Iandola, F.N., Moskewicz, M.W., Ashraf, K., Han, S., Dally, W.J., Keutzer, K., 2016. SqueezeNet: Alexnet-level accuracy with 50x fewer parameters and <1mb model size. CoRR abs/1602.07360.
- M. Lo Bianco, O. Grillo, E. Cañadas, G. Venora, G. Bacchetta, Inter- and intraspecific diversity in cistus l. (cistaceae) seeds, analysed with computer vision techniques, Plant Biology 19 (2) (2017) 183–190. doi: 10.1111/plb.12529.
- M. Lo Bianco, O. Grillo, P. Escobar Garcia, F. Mascia, G. Venora, G. Bacchetta, Morpho-colorimetric characterisation of malva alliance taxa by seed image analysis, Plant Biology 19 (1) (2017) 90–98. doi: 10.1111/plb.12481.
- A. Loddo, C.D. Ruberto, A.M.P.G. Vale, M. Ucchesu, J.M. Soares, G. Bacchetta, An effective and friendly tool for seed image analysis (2021). arXiv:2103.17213.
- Mateen, M., Wen, J., NasrullahSong, S., Huang, Z., 2019. Fundus image classification using vgg-19 architecture with pca and svd. Symmetry 11 (1). <https://doi.org/10.3390/sym11010001>.
- Mohanty, S.P., Hughes, D.P., Salathé, M., 2016. Using deep learning for image-based plant disease detection. Frontiers in Plant Science 7, 1419. <https://doi.org/10.3389/fpls.2016.01419>.
- Przybylo, J., Jabłonski, M., 2019. Using deep convolutional neural network for oak acorn viability recognition based on color images of their sections. Computers and Electronics in Agriculture 156, 490–499. <https://doi.org/10.1016/j.compag.2018.12.001>.
- Putzu, L., Di Ruberto, C., Fenu, G., 2016. A mobile application for leaf detection in complex background using saliency maps. In: Blanc-Talon, J., Distante, C., Philips, W., Popescu, D., Scheunders, P. (Eds.), Advanced Concepts for Intelligent Vision Systems. Springer International Publishing, Cham, pp. 570–581.
- Krogh Mortensen, A., Dyrmann, M., Karstoft, H., Nyholm Jørgensen, R., Gislum, R., 2016. Semantic Segmentation of Mixed Crops using Deep Convolutional Neural Network. In: CIGR-AgEng conference.
- J. Rebetez, H.F. Satizábal, M. Mota, D. Noll, L. Büchi, M. Wendling, B. Cannelle, A. Pérez-Uribe, S. Burgos, Augmenting a convolutional neural network with local histograms - A case study in crop classification from high-resolution UAV imagery, in: 24th European Symposium on Artificial Neural Networks, ESANN 2016, Bruges, Belgium, April 27–29, 2016, 2016.
- Di Ruberto, C., Putzu, L., 2014. A fast leaf recognition algorithm based on SVM classifier and high dimensional feature vector. In: Battiatto, S., Braz, J. (Eds.), VISAPP 2014 - Proceedings of the 9th International Conference on Computer Vision Theory and

- Applications, Vol. 1, Lisbon, Portugal, 5–8 January, 2014. SciTePress, pp. 601–609. doi:10.5220/0004740606010609.
- M. Sandler, A.G. Howard, M. Zhu, A. Zhmoginov, L. Chen, Mobilenetv 2: Inverted residuals and linear bottlenecks, in: 2018 IEEE Conference on Computer Vision and Pattern Recognition, CVPR 2018, Salt Lake City, UT, USA, June 18–22, 2018, IEEE Computer Society, 2018, pp. 4510–4520. doi:10.1109/CVPR.2018.00474.
- Sau, S., Ucchesu, M., Dondini, L., De Franceschi, P., D'hallewin, G., Bacchetta, G., 2018. Seed morphometry is suitable for apple-germplasm diversity-analyses. Computers and Electronics in Agriculture 151, 118–125. <https://doi.org/10.1016/j.compag.2018.06.002>.
- Sau, S., Ucchesu, M., d'Hallewin, G., Bacchetta, G., 2019. Potential use of seed morpho-colourimetric analysis for sardinian apple cultivar characterisation. Computers and Electronics in Agriculture 162, 373–379. <https://doi.org/10.1016/j.compag.2019.04.027>.
- K. Simonyan, A. Zisserman, Very deep convolutional networks for large-scale image recognition, in: Y. Bengio, Y. LeCun (Eds.), 3rd International Conference on Learning Representations, ICLR 2015, San Diego, CA, USA, May 7–9, 2015, Conference Track Proceedings, 2015.
- Sladojevic, S., Arsenovic, M., Anderla, A., Culibrk, D., Stefanovic, D., 2016. Deep Neural Networks Based Recognition of Plant Diseases by Leaf Image Classification. Computational Intelligence and Neuroscience. doi:10.1155/2016/3289801.
- C. Szegedy, W. Liu, Y. Jia, P. Sermanet, S.E. Reed, D. Anguelov, D. Erhan, V. Vanhoucke, A. Rabinovich, Going deeper with convolutions, in: IEEE Conference on Computer Vision and Pattern Recognition, CVPR 2015, Boston, MA, USA, June 7–12, 2015, IEEE Computer Society, 2015, pp. 1–9.
- C. Szegedy, V. Vanhoucke, S. Ioffe, J. Shlens, Z. Wojna, Rethinking the inception architecture for computer vision, in: 2016 IEEE Conference on Computer Vision and Pattern Recognition, CVPR 2016, Las Vegas, NV, USA, June 27–30, 2016, IEEE Computer Society, 2016, pp. 2818–2826.
- M. Ucchesu, M. Orrù, O. Grillo, G. Venora, A. Usai, P.F. Serreli, G. Bacchetta, Earliest evidence of a primitive cultivar of *Vitis vinifera* L. during the Bronze Age in Sardinia (Italy), Vegetation History and Archaeobotany 24 (5) (2015) 587–600. doi:10.1007/s00334-014-0512-9.
- A.M.P.G. Vale, M. Ucchesu, C.D. Ruberto, A. Loddo, J.M. Soares, G. Bacchetta, A new automatic approach to seed image analysis: From acquisition to segmentation, 2020. arXiv:2012.06414. [https://inspection.canada.ca/active/netapp/idseed/idseed\\_gallerye.aspx?itemsNum=1&famkey=&family=&keyword=&letter=A](https://inspection.canada.ca/active/netapp/idseed/idseed_gallerye.aspx?itemsNum=1&famkey=&family=&keyword=&letter=A), online; accessed 14 May 2021 (2020).
- X. Zhang, X. Zhou, M. Lin, J. Sun, Shufflenet: An extremely efficient convolutional neural network for mobile devices, in: 2018 IEEE Conference on Computer Vision and Pattern Recognition, CVPR 2018, Salt Lake City, UT, USA, June 18–22, 2018, IEEE Computer Society, 2018, pp. 6848–6856. doi:10.1109/CVPR.2018.00716.
- Ucchesu, M., Orrù, M., Grillo, O., Venora, G., Paglietti, G., Ardu, A., Bacchetta, G., 2016. Predictive method for correct identification of archaeological charred grape seeds: Support for advances in knowledge of grape domestication process. PLoS ONE 11 (2), doi:10.1371/journal.pone.0149814.
- Zhu, H., Yang, L., Fei, J., Zhao, L., Han, Z., 2021. Recognition of carrot appearance quality based on deep feature and support vector machine. Computers and Electronics in Agriculture 186, 106185. <https://doi.org/10.1016/j.compag.2021.106185>.